International Journal of Mechanical, Industrial and Aerospace Sciences
ISSN: 2517-9950
Vol:10, No:8, 2016

Modeling and Control of a 4DoF Robotic Assistive Device for Hand Rehabilitation

Christopher Spiewak, M. R. Islam, Mohammad Arifur Rahaman, Mohammad H. Rahman, Roger Smith, Maarouf Saad

***Abstract*—**For those who have lost the ability to move their hand, going through repetitious motions with the assistance of a therapist is the main method of recovery. We have been developed a robotic assistive device to rehabilitate the hand motions in place of the traditional therapy. The developed assistive device (RAD-HR) is comprised of four degrees of freedom enabling basic movements, hand function, and assists in supporting the hand during rehabilitation. We used a nonlinear computed torque control technique to control the RAD-HR. The accuracy of the controller was evaluated in simulations (MATLAB/Simulink environment). To see the robustness of the controller external disturbance as modelling uncertainty (±10% of joint torques) were added in each joints.

***Keywords*—**Biorobotics, rehabilitation, nonlinear control, robotic assistive device, exoskeleton.

I. Introduction

IN the United States each year more than 795,000 people suffer a stroke [1]. As many as 9 out of 10 of the survivors require rehabilitation of a varying degree [2]. Commonly affected parts are the hands which are vitally important for numerous functions as part of our daily lives. The application of a robotic assistance device in the process of rehabilitation of hand motion sees significant improvement in motor functionality recovery of the upper-limb after therapy [3]. To assist disabled individuals in the process of rehabilitation of their impaired hand motor skills, we have designed a robotic assistive device (RAD-HR). Focusing on immediate post-injury rehabilitation using a simplified design. The simplified design of the RAD-HR allows for the recovery, and rehabilitation of basic hand motion after stroke or injurie.

Compared to the conventional rehabilitation process, the use of a robotic assisted device in rehabilitation has great advantages in terms of clinical, and biomechanical measures. The use of robotic assisted devices in the rehabilitation process see a larger improvement in the Fugl-Meyer assessment of motor impairment [4]. The Fugl-Meyer assessment scale was developed as a performance based impairment index and is used as a quantitative measure of sensorimotor recover after a stroke.

The use of a robotic assisted device in rehabilitation opposed to traditional therapy sees an improvement of the direct cost-savings, and other indirect economic benefits [5]. The direct cost-savings are defined as the money spent out of pocket for the rehabilitation, and related expenses. The indirect economic benefits are defined as the improved quality of life, and the retention of the recovery.

Our RAD-HR was modelled on the average adult human hand articulations and range of movement [6]. Using the modified Denavit-Hertenberg (DH) method [7], we developed the kinematic model for the RAD-HR. In the dynamic modelling and simulation, the RAD-HR parameters such as link lengths, masses, and centroids of inertia, are estimated using the properties of a typical adult human hand [8]. The RAD-HR is designed to be worn on the forearm and the back of the hand, and was developed to provide the complete range of motion for the hand, e.g. pronation and supination, flexion and extension, and radial and ulnar movements of wrist joint; and the flexion and extension of the fingers. To maneuver the RAD-HR, a nonlinear computed torque control (CTC) technique [9] was employed in the dynamic simulation and implemented as the control system. The effectiveness of CTC to control a redundant robotic device, ETS-MARSE, was shown in our previous research [12].

In the next section of this paper, we present the kinematics, and dynamic model for the proposed RAD-HR. Details of the design, and development of the proposed RAD-HR are then presented in Section III. Section IV presents the dynamics of the RAD-HR used in the control system. Section V details the control system strategy for the proposed RAD-HR. In Section VI, simulation results are presented to evaluate the performance of the controller. Finally, the paper ends with the conclusion, and the future work in Section VII.

II. Kinematics

The kinematics for the RAD-HR was based on the modified DH method [7]. To find the modified DH parameters, we assumed that the link frames of each successive axes of rotation coincide with the joint axes of rotation and are of the same order.

The first joint, {1} (point-O in Fig. 1), is the Supination/Pronation of the arm. Joints 2, and 3 (point-A in

C Spiewak is with Biorobotics Lab, University of Wisconsin-Milwaukee, 3200 N. Cramer St., Milwaukee, USA (phone: 920-285-1605 e-mail: cjspiewak@uwm.edu).

M. R. Islam is with Biorobotics Lab, University of Wisconsin-Milwaukee, 3200 N. Cramer St., Milwaukee, USA (e-mail: islam4@uwm.edu).

M. A Rahaman is with the Mechatronics Lab, Khulna University of Engineering & Technology, Khulna Bangladesh, (e-mail: rahaman.arifur02@gmail.com).

M. H. Rahman is with Mechanical/Biomedical Engineering Department, University of Wisconsin-Milwaukee, 3200 N. Cramer St., Milwaukee, USA (e-mail: rahmanmh@uwm.edu).

R. Smith is with Department of Occupational Science & Technology, University of Wisconsin-Milwaukee, Milwaukee, USA (e-mail: smithro@uwm.edu).

M. Saad is with Département de Génie Électrique, École de technologie supérieure, Montréal, Canada (e-mail: maarouf.saad@etsmtl.ca).

Fig. 1) together constitute the wrist joint. Joint 2 is the flexion and extension of the wrist, and joint 3 is the radial and ulnar deviation of the wrist. Joint 4 (point-B in Fig. 1) is then the combined flexion and extension of the four fingers.

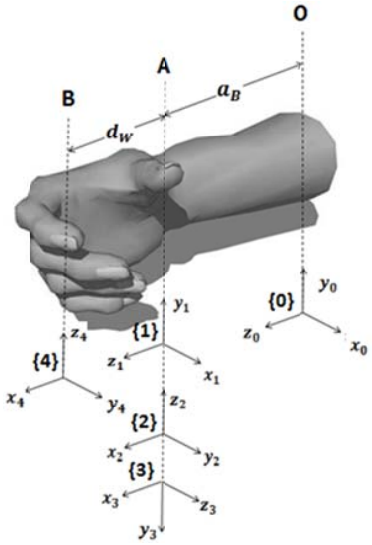

Fig. 1 Link frame assignments

TABLE I
MODIFIED DH PARAMETERS

Joint (i)	α_{i-1}	d_i	a_{i-1}	θ_i
1	0	d_W	0	θ_1
2	-π/2	0	0	θ_2
3	-π/2	0	0	θ_3
4	π/2	0	a_B	θ_4

The modified DH parameters of the link frame assignments are summarized in Table I. These parameters are used to represent the positions and orientations of the frames with respect to the fixed reference frame, {0} (point-O in Fig. 1). Consider that the fixed frame of reference {0} is located at a distance a_B from the frame {2} (at point-A in Fig. 1). General form of a link transformation that relates frame $\{i\}$ to the frame $\{i\text{-}1\}$ [7] is expressed in (1).

$$ {}^{i-1}_{i}T = \begin{bmatrix} {}^{i-1}_{i}R^{3\times3} & {}^{i-1}_{i}P^{3\times1} \\ 0^{1\times3} & 1 \end{bmatrix} \quad (1) $$

$$ {}^{i-1}_{i}R = \begin{bmatrix} cos\,\theta_i & -sin\,\theta_i & 0 \\ sin\,\theta_i\,cos\,\alpha_{i-1} & cos\,\theta_i\,cos\,\alpha_{i-1} & -sin\,\alpha_{i-1} \\ sin\,\theta_i\,sin\,\alpha_{i-1} & cos\,\theta_i\,sin\,\alpha_{i-1} & cos\,\alpha_{i-1} \end{bmatrix} \quad (2) $$

$$ {}^{i-1}_{i}P = [a_{i-1} \quad -sin\,\alpha_{i-1}\,d_i \quad cos\,\alpha_{i-1}d_i]^T \quad (3) $$

where ${}^{i-1}_{i}R$ is the rotation matrix that describes the frame $\{i\}$ in relation to the previous frame $\{i\text{-}1\}$. Additionally, ${}^{i-1}_{i}P$ is the vector of the origin of frame $\{i\}$ relative to the previous frame $\{i\text{-}1\}$. The positions and orientations of the reference frame attached to the finger joint {4} with respect to the fixed reference frame {0} can then be obtained by multiplying the individual transformation matrices.

III. Design of the Assistive Device

The RAD-HR (Fig. 2) uses the basic biomechanical behaviors of an average human hand to simplify the design. This allows us to focus on the main motions desired to recover. The RAD-HR is limited to the pronation and supination of the forearm, the two joints of the hand and additionally the fingers. The two main joints are where the four fingers attach to the hand (point-B in Fig. 1), and the wrist (point-A in Fig. 1). These joints have been restricted in there range of motion for patient safety, specified in Table II [10], [11]. The motion is restricted mostly by limiting the physical capabilities of the RAD-HR to ranges less than that of an average healthy humans ranges of motion in their hand.

The RAD-HR attaches to the forearm, palm, thumb, and fingers. Three micro linear servos were used to actuate the RAD-HR in order to help move the hand appropriately. One actuator is placed on the back of the hand to operate the flexion and extension of the fingers. The flexion and extension of the fingers manipulates a separate sub-mechanism which is attached to the thumb. When the fingers go into flexion the thumb will also and vice versa. There are then two servos mounted on top of the forearm which aid in the flexion and extension (both of them extend fully, or retract to half extension), and the radial and ulnar deviation (one extends fully one retracts fully) of the wrist, and one actuator for pronation and supination of the forearm as well.

The RAD-HR is designed to be worn on the forearm and the back of the hand. The device is supposed to be attached with the hand by soft wrist strap. Then, it will be mounted on an arm support (Fig. 3) that will help to hold the arm stable while going through exercises.

TABLE II
RANGES OF MOTION AND LIMITING RANGES FOR THE RAD-HR

	Motion	Average Human [8]	RAD-HR
Wrist	Radial Deviation	20°	22°
	Ulnar Deviation	30°	22°
	Flexion	70°	90°
	Extension	90°	90°
Fingers	Flexion/Extension	90°	90°
Forearm	Supination/Pronation	90°	90°

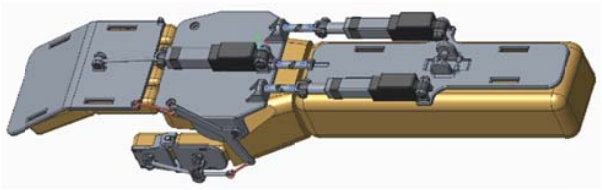

Fig. 2 RAD-HR attached to a simplified hand-forearm model

This base holds the arm at a slight incline to allow full operation of the RAD-HR. The RAD-HR simply slides into the arm swivel in the center. The arm swivel is controlled by a servo motor which is mounted underneath. This allows for the supination and pronation of the arm to better facilitate the rehabilitation process.

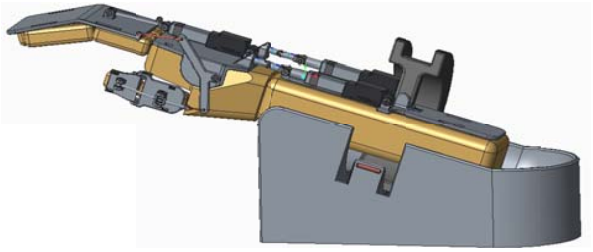

Fig. 3 RAD-HR mounted on a base/arm rest

IV. Dynamics

The dynamic behaviour of the RAD-HR can be modelled as follows by the rigid body dynamic equation:

$$\tau = M(\theta)\ddot{\theta} + V(\theta,\dot{\theta}) + G(\theta) \quad (4)$$

where $\theta \in \mathbb{R}^4$ is the joint variables vector, $\tau \in \mathbb{R}^4$ is the generalized torques vector, $M \in \mathbb{R}^{4\times4}$ is the inertia matrix, $V(\theta,\dot{\theta}) \in \mathbb{R}^4$ is the Coriolis/centrifugal vector, and $G(\theta) \in \mathbb{R}^4$ is the gravity vector. However, this is only in an ideal setting. Therefore, to take into account the modeling uncertainty, an external disturbance as noise is added in the dynamic modeling of the RAD-HR. Therefore, (4) can be written as:

$$\tau = M(\theta)\ddot{\theta} + V(\theta,\dot{\theta}) + G(\theta) - \tau_n \quad (5)$$

$$\ddot{\theta} = -M^{-1}(\theta)\left[V(\theta,\dot{\theta}) + G(\theta)\right] + M^{-1}(\theta)(\tau + \tau_n) \quad (6)$$

$M^{-1}(\theta)$ always exists since $M(\theta)$ is symmetrical and positive definite.

V. Control

To manage, direct, and regulate the behaviour of the RAD-HR, we have employed nonlinear computed torque control technique. A schematic diagram of the CTC for RAD-HR is shown in Fig. 4. The CTC allows us to adjust for error in the trajectory tracking as it is being created.

The error vector, E, and its derivatives are defined as:

$$\ddot{E} + K_d\dot{E} + K_pE + K_i\int E dt = M(\theta)^{-1}\tau_n \quad (7)$$

where the terms θ_d, $\dot{\theta}_d$, and $\ddot{\theta}_d$ symbolize the desired angular position, velocity, and acceleration, respectively. The terms K_p, K_d, and K_i are represent positive definite diagonal matrices of the proportional, derivative, and integral gains. The proportional coefficient, K_p, corrects for the present values of error. The integral coefficient, K_i, corrects for the past values of error. The derivative coefficient, K_d, adjusts for the possible future error values.

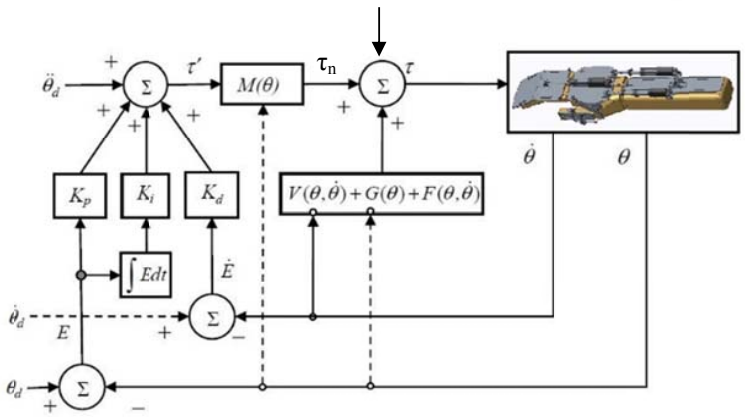

Fig. 4 Schematic diagram of Computed Torque Control

VI. Simulation

To see the performance of our CTC system that we developed for our RAD-HR, firstly we simulated an exercise representing individual joint movement (Fig. 5) and secondly an exercise with multi-joint movement of hand which basically mimicked pick and drop a target (Fig. 6). The later one is that the RAD-HR with its base should be kept on a table and subject would try to pick a target from left and drop it on right, then it would return its initial position. Therefore, it requires forearm pronation and supination, wrist flexion and extension, wrist radial and ulnar deviation, and fingers flexion and extension to be executed simultaneously. The simulation used generated trajectories which correspond to these two types of movement. In practice, there might be unwanted disturbance, modeling errors, or noise, therefore simulation was carried out with ±10% disturbance in the joints.

Fig. 5 depicts the simulated result for individual joint movement of subject's hand whereas Fig. 6 shows the result for multi-joint movement. The simulation plots generated originally with a reference trajectory (Figs. 5 and 6; dotted line in the first row of the plots), or the desired motion, and the measured or the outcome of the simulation (Figs. 5 and 6; solid line in the first row of the plots) of the CTC system. As we see from Figs. 5 and 6, the desired and measured trajectories are almost overlapped and indistinguishable for each case that depicts how closely the reference trajectory is followed by. The reason behind this is that simulation for either cases produce very low error ($< 0.25^{\circ}$, error vs. time

plots in Figs. 5, and 6) which advocates the efficiency and robustness of controller that we developed. In spite of having noise in each joint, CTC is capable enough to follow the desired trajectory. However, required torques to move the joints are also plotted against time. In Fig. 5, torque (red line) and noise (blue line) is shown for every joint and the amount of torque is pretty much low which indicates that RAD-HR would need low energy.

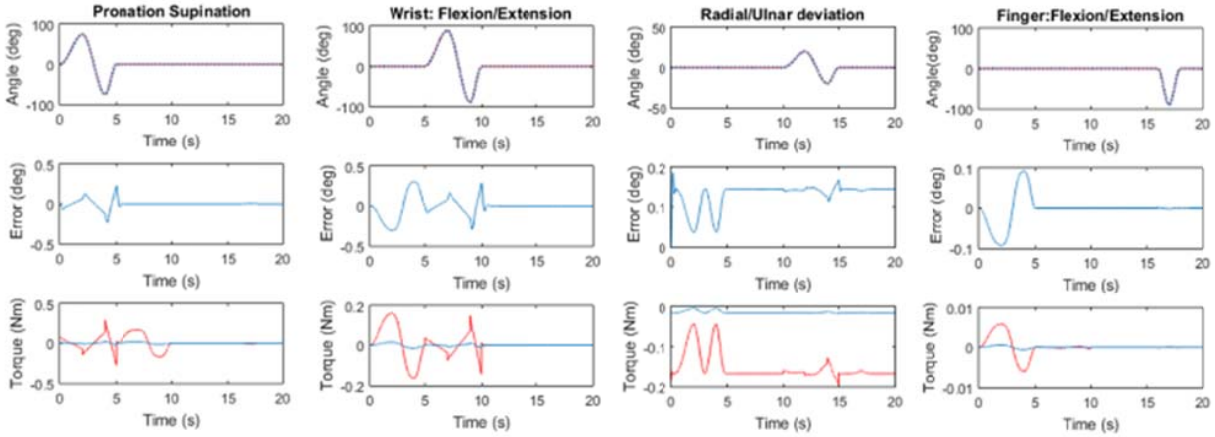

Fig. 5 Simulated result, individual joint movement

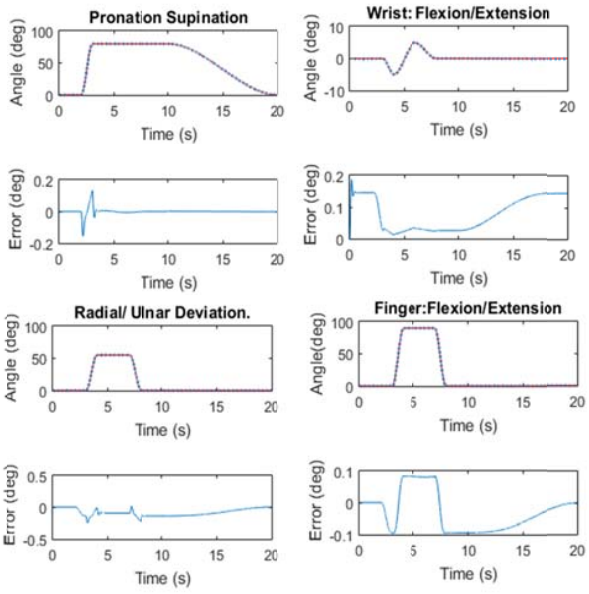

Fig. 6 Simulated result for multi joint movement

VII. Conclusion

The kinematic and dynamic model of the RAD-HR corresponds to the healthy range of motion for an average human hand is presented. The nonlinear computed torque control technique used in the dynamic simulation properly tracks trajectory corresponding to the typical passive rehabilitation exercises. Using the developed base gives support to the RAD-HR and limb of the subjects giving way to ease of use.

Future work looks to develop, and fine tune the software backend along with improving the ergonomic of the design. Later moving into non-clinical trials tested the ease of use.

Acknowledgment

The first author gratefully acknowledges the support provided for this research through McNair, and SURF scholarships.

References

[1] D. Mozaffarian, E. J. Benjamin, A. S. Go, D. K. Arnett, M. J. Blaha, M. Cushman, S. R. Das, S. de Ferranti, J. P. Després, H. J. Fullerton, and V. J. Howard, "Heart Disease and Stroke Statistics—2016 Update A Report from the American Heart Association," *Circulation*, CIR-0000000000000350, 2015.

[2] "Paralysis," *Stroke.org*, 2014. (Online). Available at: http://www.stroke.org/we-can-help/survivors/stroke-recovery/post-stroke-conditions/physical/paralysis. (Accessed: 06-Mar-2016).

[3] S. Masiero, A. Celia, G. Rosati, and M. Armani, "Robotic-assisted rehabilitation of the upper limb after acute stroke," *Archives of physical medicine and rehabilitation,* vol. 88, no. 2, pp. 142-9, 2007.

[4] P. S. Lum, C.G. Burgar, P. C. Shor, M. Majmundar, and M. Van der Loos, "Robot-Assisted Movement Training Compared with Conventional Therapy Techniques for the Rehabilitation of Upper-Limb Motor Function After Stroke," *Archives of Physical Medicine and Rehabilitation,* vol. 83, no. 7, pp. 952-959, 2002.

[5] G. R. Romer, H. J. Stuyt, and A. Peters, "Cost-savings and economic benefits due to the assistive robotic manipulator (ARM)," in *9th International Conference on Rehabilitation Robotics,* ICORR, 2005, pp. 201-204.

[6] A.D. Winter, Biomechanics and Motor Control of Human Movements, 2nd ed., University of Waterloo Press, Canada, 1992.

[7] J. J. Craig, Introduction to Robotics Mechanics and Control, 3rd ed.: Pearson Prentice Hall, 2004.

[8] N. P. Hamilton, *Kinesiology: Scientific basis of human motion.* Brown & Benchmark, 2011.

[9] D. J. Magee, J. E. Zachazewski, and W. S. Quillen, *Pathology and intervention in musculoskeletal rehabilitation*. Elsevier Health Sciences, 2008.

[10] M H. Rahman, M. Saad., J-P Kenné, and P. S. Archambault (2013). "Control of an Exoskeleton Robot Arm with Sliding Mode Exponential Reaching Law." International Journal of Control, Automation, and Systems ,201, vol. 11 no 1: pp 92-104.

[11] Chen M, SK Ho, HF Zhou, PMK Pang, XL Hu, Ng DTW, Tong KY:Interactive rehabilitation robot for hand function training. In Proc. IEEE International Conference on Rehabilitation Robotics ICORR.Kyoto, Japan; 2009:777–780.

[12] M. H. Rahman, M. J. Rahman, O. L. Cristobal, M. Saad, J. P. Kenné and P. S. Archambault " Development of a whole arm wearable robotic exoskeleton for rehabilitation and to assist upper limb movements." Robotica CJO 2014, doi:10.1017/S0263574714000034.